Quantum/Classical Investigation of Amide Protonation in Aqueous Solution

Dirk Zahn,[†,‡] Karl Friedemann Schmidt,[‡] Stefan M. Kast,[‡] and Jürgen Brickmann*[,‡,§]

Physikalische Chemie I, Technische Universität Darmstadt, Petersenstraβe 20, D-64287 Darmstadt, Germany

Received: July 24, 2001; In Final Form: April 25, 2002

The protonation of *N*-methylacetamide by a hydronium ion is investigated by means of ab initio methods and statistical-mechanical integral equation theory. The proton-transfer reaction is treated as a function of a two-dimensional coordinate. It is monitored in terms of the distance of the transferred proton to the amide oxygen atom and the distance of the oxygen atoms of the amide and the hydronium. The energy profile of the reaction is calculated for the isolated system as well as for the reaction in aqueous solution. The reaction in a vacuum is investigated by ab initio calculations. The solvent effect is modeled on the basis of a classical approach using the reference interaction site model integral equation theory. Therein reactant and product states are described by classical force fields. A smooth transition between both states is modeled using a continuous switching function. The proton-transfer potential was calculated for the average solvent effect. As a result, the minimum energy path for amide protonation is determined as a function of a one-dimensional reaction coordinate.

1. Introduction

Protic catalysis is known to enhance the speed of peptide hydrolysis by several orders of magnitudes. The first step in acid catalyzed peptide hydrolysis is the protonation of an amide group. The most favorable site for protonation is commonly believed to be the carbonyl oxygen atom.[1] Because of the great importance of peptide hydrolysis, peptide protonation was investigated in a number of theoretical works. The ab initio studies were mostly based on the proton affinities.[2,3] Such considerations only include two states of the protonation reaction, reactant and product state. In the present work, proton transport from a hydronium ion to a model peptide is investigated by means of ab initio calculations. Therein, the proton-transfer potential is calculated as a continuous function of a two-dimensional coordinate.

The reaction is investigated in a vacuum as well as in aqueous solution. The solvent may have a significant effect on proton-transfer reactions. For example, the most stable configuration of a protonated water dimer in a vacuum is the symmetric $H_5O_2^+$ complex.[4,5] In aqueous solution however, the excess proton is preferably associated to a single water molecule.[6] Although ab initio calculations may easily be performed for isolated systems, the treatment of a solvent is more sophisticated.

Including explicit solvent molecules into the quantum chemical calculations seems to be a straightforward approach. This, however increases the numerical costs dramatically. Computationally more feasible but less accurate are continuum methods. In hybrid quantum/classical approaches, only a subset of the system coordinates is treated quantum mechanically. Usually, the modes which are considered as the most relevant for the desired investigations are treated quantum mechanically, whereas the other degrees of freedom are investigated by less accurate but computationaly more efficient classical methods.

In this paper, we report a quantum/classical model of proton transport to *N*-methylacetamide (NMAA) in a vacuum as well as in aqueous solution. Therein, the amide group of NMAA is taken as a model for the amide group of a peptide. The reaction in a vacuum is treated in a quantum picture. The reactants are the model peptide and a hydronium ion approaching the carbonyl group of NMAA (Figure 1). Only for this system, a quantum mechanical description is chosen.

The reaction in solution is investigated on the basis of a quantum/classical model. Therein the solvent molecules are treated as classical particles. For both reactant and product state, the interaction of solvent molecules may be modeled with sufficient accuracy by classical force fields. For the intermediate states, an approximate force field is obtained from interpolation of reactant and product force fields. The solvent configurational space and the solute−solvent statistics are described by reference interaction site model (RISM)[7] integral equation theory. On the basis of this model, the average solvent effect may be computed at very low costs. However, nonequilibrium effects may not be investigated and are not considered in this paper.

This paper is structured as follows. In the next section, the quantum/classical approach is described. Section 3 deals with the details of the methods used. Our results are reported in section 4 and summarized in the final section.

2. Theory

2.1. The Model System. As a model for proton transport to the oxygen atom of an amide group in aqueous solution, a protonated complex of NMAA and a water molecule are investigated (see Figure 1). The proton-transfer reaction is described by a two-dimensional coordinate: the distance of the oxygen atoms R_{OO} and the distance of the transferring proton to the carbonyl oxygen r_H.

2.2. Proton-Transfer Potential. The proton-transfer potential in solution V_{solv} may be written as the sum of the transfer

* To whom correspondence should be addressed. Phone: (+49) 6151-162198. Fax: (+49) 6151-164298. E-mail: brick@pc.chemie.tu-darmstadt.de.

† Present address: CSCS/ETH Zürich, Via Cantonale, CH-6928 Manno, Switzerland.

‡ Technische Universität Darmstadt.

§ Darmstädter Zentrum für wissenschaftliches Rechnen (DZWR).

10.1021/jp012830k CCC: $22.00
Published on Web 08/06/2002

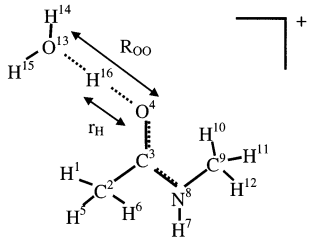

Figure 1. [*N*-methylacetamide··H^+··H_2O] complex.

potential in a vacuum V_{vac} and a solvent term V^S:

$$V_{solv} = V_{vac} + V^S \tag{2.1}$$

The vacuum term is obtained from ab initio calculations and is taken as a function of the distance of the oxygen atoms R_{OO} and the distance of the transferring proton to the carbonyl oxygen r_H. The solvent term is a function of all coordinates of the system. To model this term, we chose an approach which is based on the interpolation of the potentials V_R^S and V_P^S of the reactant and the product state. Both reactant and product energy terms are described by classical force fields including Lennard-Jones and Coulomb terms, which are described in the next section. The interpolation is accomplished by introducing a switching function w_R which allows a smooth transition from reactant to product state:

$$V^S = w_R V_R^S + (1 - w_R) V_P^S \tag{2.2}$$

This approach was successfully applied to proton transfer in water[8−10] and is now transferred to amide protonation in aqueous solution.

The most important effect of the aqueous solvent on the proton transfer is its Coulomb interaction with the reacting molecules.[8−10] It is therefore reasonable to parametrize the switching function in accordance to the charge distribution of the [NMAA··H^+··H_2O]− complex. The dipole moment was obtained from the ab initio treatments as a function of the coordinates r_H and R_{OO}. From this, the switching function is determined by fitting the dipole moment given by the interpolation of the partial charges taken from the reactant (q_i^R) and the product (q_i^P) force fields to the dipole moment derived from the ab initio calculations. Thus, the interpolated charges q_i read:

$$q_i = w_R q_i^R + (1 - w_R) q_i^P \tag{2.3}$$

Here the q_i^R and the product q_i^P are taken form force field parameters. Formally the dipole moment is given by

$$\boldsymbol{\mu}(\text{forcefield}) = \sum_i \mathbf{r}_i q_i, \quad \mu_{OO}(\text{forcefield}) = \sum_i \mathbf{r}_i \cdot \mathbf{e}_{OO} q_i \tag{2.4}$$

where i denotes the index of the atoms at position $\mathbf{r}_i$ as obtained from the ab initio geometry optimizations. The unit vector $\mathbf{e}_{OO}$ is chosen to point from the oxygen atom of NMAA to the water oxygen atom. To determine w_R from eqs 2.3 and 2.4, only the component of the dipole moment along the axis between the oxygen atoms μ_{OO}(force field) was considered. We demand the dipole moment μ_{OO}(force field) of the complex according to the interpolated force field charges to be equal to the dipole moment μ_{OO}(ab initio) obtained from the ab initio calculations. The switching function then results as

$$w_R = \frac{\mu_{OO}(\text{abinitio}) - \sum_i \mathbf{r}_i \cdot \mathbf{e}_{OO} q_i^P}{\sum_i \mathbf{r}_i \cdot \mathbf{e}_{OO} (q_i^R - q_i^P)} \tag{2.5}$$

For convenience, the functional form of the switching function is taken, in analogy to investigations of proton transfer in water,[8−10] as

$$w_R(r_H, R_{OO}) = \frac{1}{2}\{1 - \tanh[a(r_H - b)]\} \tag{2.6}$$

On the basis of eqs 2.5 and 2.6, the actual values of a and b may be parametrized as functions of the oxygen distance R_{OO} in the complex.

It is noteworthy that the interpolation function w_R is only a function of the coordinates of the reactants and the products. The potential defined in eq 2.2 may be easily computed during molecular dynamics or Monte Carlo simulations and is thus particularly useful for mixed quantum/classical approaches. As in refs 8−10, the model for the solvent term V^S of the proton-transfer potential V_{solv} in principle may be used for any solvent situation. However, in the present work, we will only elucidate the average solvent effect on the proton-transfer reaction.

2.3. Solvent Model. The calculation of thermodynamic quantities of molecular solvation requires, in general, very extensive simulation. There is a strong need for more effective procedures. In the present work, the solvent was modeled by the reference interaction site (RISM) integral equation method,[7] which models molecular interactions by pairwise additive atomic potentials. We used the well-known matrix form of the RISM integral equations for a molecular fluid, which have first been invented by Chandler and co-workers.[11] The RISM integral equations provide a statistical solvent model resulting a radially averaged description of the solvent structure which depends on the conformation of solute molecules. Although the distribution functions are approximate, the structural results were found to agree reasonably well with simulation data for pure liquids[12,13] and for solutions.[14−19] Furthermore, the energy of solvation for a solute molecule can be determined quickly from the solution of the integral equations for a given solute geometry.

The RISM integral equations reduce the 3D distribution of the solvent to radial site−site pair correlation function matrixes **h**, which take the forms

$$\mathbf{h}^{vv} = \omega^v * \mathbf{c}^{vv} * (\omega^v + \rho \mathbf{h}^{vv}) \tag{2.7}$$

$$\mathbf{h}^{uv} = \omega^u * \mathbf{c}^{uv} * (\omega^v + \rho \mathbf{h}^{vv}) \tag{2.8}$$

The dimensionality of the matrixes equals to the number of solute or solvent interaction sites, which are denoted by u and v, respectively. Here, ρ is the number density of the solvent molecules, and **c** is the matrix of intermolecular direct correlation functions. The star (*) denotes matrix convolution products. $\boldsymbol{\omega}$ is the matrix of intramolecular pair correlation functions with the elements

$$\omega_{jk}(\mathbf{r}) = (1 - \delta_{jk}) \frac{\delta(|\mathbf{r}| - |\mathbf{d}_{jk}|)}{4\pi |\mathbf{d}_{jk}|^2} \tag{2.9}$$

as functions of the bond length $|\mathbf{d}_{jk}|$. Each solvent molecule is considered as a set of N atomic sites j, k, interacting via the site−site pair potential $U(r)$, which is given by the sum of a

short-ranged Lennard-Jones and a long-ranged Coulomb term:

$$U_{jk}(r) = U_{jk}^{LJ}(r) + U_{jk}^{C}(r) = 4\pi\epsilon_{jk}\left[\left(\frac{\sigma_{jk}}{r}\right)^{12} - \left(\frac{\sigma_{jk}}{r}\right)^{6}\right] + \kappa\frac{q_j q_k}{4\pi\epsilon_0 r} \tag{2.10}$$

The partial charges on the atomic interaction sites j, k are denoted by q_i, q_k. The interatomic short-range parameters are obtained by the Lorentz−Berthelot rules:[7]

$$\sigma_{jk} = \frac{\sigma_j\sigma_k}{2}\epsilon_{jk} = \sqrt{\epsilon_j\epsilon_k} \tag{2.11}$$

To take account for accurate screening of the long-range interaction, the RISM-screened solvent intermolecular Coulomb potential is replaced by a phenomenological result:[20]

$$\kappa = \begin{cases} \left[\dfrac{(\epsilon_r - 1)k_B T + \frac{4}{3}\epsilon_0\pi\rho\mu_{RISM}^2}{(\epsilon_r - 1)\cdot\frac{4}{3}\pi\rho\mu_{RISM}^2}\right] & \text{; solvent - solvent interaction} \\ 1 & \text{; solute − solvent interaction} \end{cases} \tag{2.12}$$

where μ_{RISM} is the dipole moment of the solvent molecule according to its point charges as derived from the OPLS force field (see chapter 3), ϵ_0 is the vacuum dielectric constant, ϵ_r is the phenomenological dielectric constant at the absolute temperature T, and k_B is the Boltzmann constant.

A closure equation is needed to solve eqs 2.7 and 2.8. Among various closures discussed in the literature,[7,20−22] the hypernetted chain approximation supplies a closed expression of the chemical potential which has been shown to describe polar fluids with a reasonable degree of accuracy:[12−19]

$$h_{jk} = \exp\left(-\frac{U_{jk}}{k_B T} + h_{jk} - c_{jk}\right) - 1 \tag{2.13}$$

Equations 2.7, 2.8, and 2.13 form a set of coupled nonlinear integral equations which was used to calculate correlation functions of liquids with respect to the temperature and the density of the solvent. From the set of solute−solvent correlation functions, energies of solvation $V_{R,P}^{S}$ were derived by eq 2.14:

$$V_{R,P}^{S} = -4\pi\rho\sum_j\sum_k\left[\int r^2[U_{jk}(h_{jk} + 1)]\,dr\right] \tag{2.14}$$

Free energies of solvation ΔG^S were calculated according to expression 2.15,[23] which includes Gaussian statistics of the solvent bath:

$$\Delta G^S = -4\pi\rho k_B T\sum_j\sum_k\left[\int r^2(-c_{jk} + 0.5h_{jk}c_{jk})\,dr\right] \tag{2.15}$$

This form for the free energy of solvation has been shown to yield free energies in reasonable agreement with simulation and experimental data.[17]

3. Methods

The ab initio calculations were carried out with the Gaussian 94 software package[24] using a 6-311G** basis set and the B3LYP[25,26] density functional. The B3LYP density functional was chosen for reasons of comparability to Car-Parrinello simulations of this reaction, which will be presented in a forthcoming publication. For the exploration of the proton-transfer potential, a set of geometry optimization runs were performed. Therein, the oxygen distance R_{OO} was constrained at 2.3, 2.5, 2.7, and 3.0 Å (Figure 1). The transferring proton was initially placed at a distance of 1.0 Å from the carbonyl oxygen. The product state was determined by geometry optimization. Therein, only the oxygen distance was kept fixed. To explore the transfer potential, the proton was moved from reactant to product state by imposing additional constraints on the distance of the proton and the oxygen atom of the water molecule. The proton was moved in steps of 0.1 Å up to a distance of 0.9 Å to the water oxygen atom. Finally, a further geometry optimization was done without constraining the proton position. Thereby, possible local minima corresponding to the reactant states were investigated.

The solvent distribution functions were calculated on the basis of the optimized potential for liquid simulations (OPLS) force field.[27] For the water molecules, a slightly modified TIP3P model[28] was applied, which includes additional Lennard-Jones terms for the hydrogen atoms. This modification is used to avoid Coulomb fusion which otherwise arises inevitably during RISM calculations. As in previous studies,[29] the corresponding σ_H was chosen as 0.4 Å, far less than σ_O. Thus, the additional potential has a negligible effect on the total interaction of the water molecules.

We used the HNC closure to solve the RISM integral equations on a logarithmic grid of 512 points, screening the distribution functions within the interval [0.00598 Å, 164 Å]. For the calculation of Fourier transforms of the distribution functions, the Talman method[30] was used. A damped iterative Picard procedure[7] was employed to converge the distribution functions. The calculations were repeated until the maximum change in all direct correlation functions met the convergence criterion $\max(\Delta c_{jk}) < 10^{-5}$.

The force field for the hydronium ion was adopted from Voth et al.[31] For the protonated amide, a new force field was generated. The Lennard-Jones coefficients were taken from the OPLS parameter list. The partial charges q_i(OPLS) as listed in OPLS were modified according to the change in partial charges Δq_i(ab initio) caused by protonation of the amide. The charge correction was determined from comparing the charge distributions of the amide and its protonized form as obtained from ab initio calculations. The ab initio partial charges were evaluated on the basis of the electrostatic potential derived charges model:

$$q_i^{HNMAA^+} = q_i^{NMAA}(\text{OPLS}) + \Delta q_i^{HNMAA^+}(\text{abinitio}) \tag{3.1}$$

where i denotes the index of the atoms of the amide.

All force field parameters are listed in Table 1. The corresponding indices of the atoms are indicated in Figure 1.

4. Results

The potential energy surface for proton transfer within the isolated complex was calculated as a function of the oxygen distance R_{OO} and the distance r_H of the transferring proton to the carbonyl oxygen atom. The resulting data was used for fitting interpolating polynomials. These were chosen to be of the type

$$V_{vac} = \sum_{j=1}^{4} a_j(R_{OO})r_H^{\,j-1} \tag{4.1}$$

Therein, the information about local minima was explicitly included in order to exactly reproduce the minima of the transfer potential by the interpolating polynomials. Thus, some of the

TABLE 1: Force Field Parameters for Reactant and Product State for the Protonation of NMAA in Aqueous Solution[a]

	reactants			products		
atom	q_i/e	σ/Å	ϵ/kcal mol^{-1}	q_i/e	σ/Å	ϵ/kcal mol^{-1}
H^1	0.0600	2.5000	−0.0300	0.0907	2.5000	−0.0300
C^2	−0.1800	3.5000	−0.0660	−0.1066	3.5000	−0.0660
C^3	0.5000	3.7500	−0.1050	0.3697	3.7500	−0.1050
O^4	−0.5000	2.9600	−0.2100	−0.3868	3.1200	−0.1700
H^5	0.0600	2.5000	−0.0300	0.0907	2.5000	−0.0300
H^6	0.0600	2.5000	−0.0300	0.1255	2.5000	−0.0300
H^7	0.3000	0.5000	−0.0300	0.3390	0.5000	−0.0300
N^8	−0.5000	3.2500	−0.1700	−0.3064	3.3000	−0.1700
C^9	0.0200	3.5000	−0.0660	−0.0926	3.5000	−0.0660
H^{10}	0.0600	2.5000	−0.0300	0.1494	2.5000	−0.0150
H^{11}	0.0600	2.5000	−0.0300	0.1191	2.5000	−0.0150
H^{12}	0.0600	2.5000	−0.0300	0.1494	2.5000	−0.0150
O^{13}	−0.4166	3.1508	−0.1521	−0.8340	3.1508	−0.1521
H^{14}	0.4722	0.4000	−0.0460	0.4170	0.4000	−0.0460
H^{15}	0.4722	0.4000	−0.0460	0.4170	0.4000	−0.0460
H^{16}	0.4722	0.4000	−0.0460	0.4589	0.5000	−0.0300

[a] The indexing of the atoms is the same as in Figure 1.

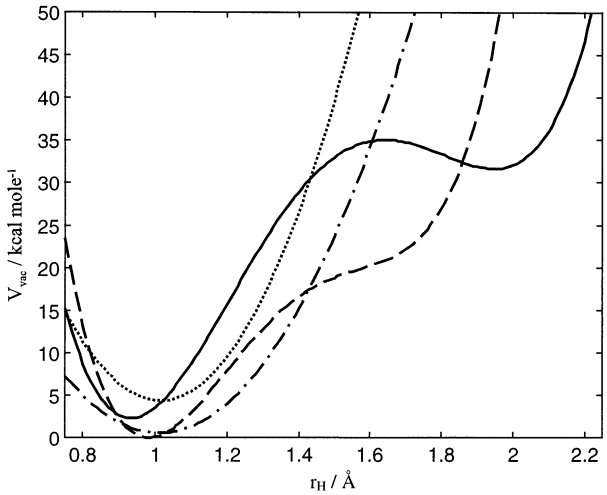

Figure 2. Potential energy surface for proton transport in a vacuum as a function of the distance of the transferring proton to the carbonyl oxygen atom for selected oxygen distances (R_{OO}: 3.0, 2.7, 2.5, and 2.3 Å: solid, dashed, dash−dotted, and dotted lines).

coefficients a_j were eliminated using

$$\frac{\partial}{\partial r_H} V_{vac}|_{r_H}^{min} = 0 \tag{4.2}$$

where r_H^{min} denotes the local minima. The resulting interpolated potential energy curves are shown in Figure 2. The polynomial coefficients as well as the root-mean-square errors of the interpolation procedure are listed in Table 2a. To provide a two-dimensional potential energy surface, we interpolated the parameters a_1, .., a_4 as functions of the oxygen distance:

$$a_j = \sum_{k=1}^{4} b_k^j R_{OO}^{k-1} \tag{4.3}$$

The corresponding interpolation coefficients are listed in Table 2b. The quartic fits are well suited for describing the potential energy curves for proton transfer between the oxygen atoms of the two molecules. This includes the potentials minima as well as the proton-transfer barriers. However, for the asymptotic behavior of the potential at small (<0.9 Å) and large r_H, one may expect deviations of the extrapolated curve from the real potential. These values of r_H correspond to situations in which the proton is at very short distance to one of the oxygen atoms. Because this short-range region is of no relevance for proton transfer, it was not studied in more detail.

According to Figure 2, the proton is preferable associated to the carbonyl oxgen atom. The energy difference between reactant and product state for the vacuum reaction was found to be up to 30 kcal/mol. It must be pointed out that the potential is only parametrized for proton transfer between the two oxygen atoms.

In the following, the solvent effect on the proton-transfer potential is investigated. For this purpose, we first determine the interpolation function used in eq 2.2.

The switching function w_R for modeling the transition from reactant to product state was calculated according to eqs 2.3 and 2.6. The parameters a and b related to w_R can be described as a function of the oxygen distance R_{OO}. The corresponding polynomial reads:

$$a = 3.395\ \text{Å}^{-1} - 0.6694\ \text{Å}^{-2} R_{OO} \tag{4.4a}$$

$$b = 0.03743\ \text{Å} + 0.4428 R_{OO} \tag{4.4b}$$

The switching function is plotted for two selected oxygen distances in Figure 3. Therein, the circles mark the data points obtained from the ab initio calculations. The root-mean-square error for describing the data according to all oxygen distances with the fitted function is 1.1×10^{-3}.

The switching function was then used for modeling the solvent effect on the protonation of NMAA in aqueous solution. The resulting potential energy surface is shown in Figure 4. Like for the isolated system, the proton transfer potential in aqueous solution also exhibits a preference of peptide protonation. However, the energy gap between reactant and product state is much lower than it was found for the vacuum reaction (Figure 2).With regard to only the interaction of the surrounding water molecules, the reactant state was found to be strongly favored over the product states. This weakens the amides basicity in comparison to the gas phase, but the proton is still preferably associated to the NMAA. For oxygen distances of 2.7 and 3.0 Å, the global minimum of the proton-transfer potential may be related to the protonated state of the amide. For both curves, we found local minima corresponding to the deprotonated amide. At an oxygen distance of 2.3 Å, only one minimum can be seen. The location of this minimum is roughly in the middle between the two oxygen atoms. We therefore expect the proton to be shared between both oxygen atoms. We interpret the curve for the oxygen distance of 2.5 Å as an intermediate between those for the short oxygen distance of 2.3 Å, favoring a shared proton and the greater oxygen distances for which the minima may be related to the protonated and deprotonated amide. At 2.5 Å, the global minimum of the transfer potential may be related to an (unequally) shared proton and the local minimum corresponds to the deprotonated amide. We assume the shoulder on the left indicates the formation of a minimum according to the protonated amide. However, a more accurate solvent treatment would be required for further investigation of such a phenomenon.

Finally, we investigated the minimum energy path of the transfer reaction. The corresponding potential energy curve is shown in Figure 5a. For the most favorable product state, the distance r_H of the transferring proton to the carbonyl oxygen atom was found to be 0.97 Å. The transition state is located at $r_H = 1.67$ Å. The local minimum on the reactant side was found at $r_H = 2.06$ Å. The energy difference between the minima of

TABLE 2: (a) Coefficients of the Interpolation Polynomials for the Proton Transfer Potential in Vacuum as a Function of the Oxygen Distance R_{OO} and (b) Coefficients of the Interpolation Polynomials for the Parameters a_0, ..., a_4

(a)

R_{OO}	a_0/ kcal mol^{-1}	a_1/ kcal mol^{-1} Å^{-1}	a_2/ kcal mol^{-1} Å^{-2}	a_3/ kcal mol^{-1} Å^{-3}	a_4/ kcal mol^{-1} Å^{-4}	rms/ 10^{-3} kcal mol^{-1}
2.3	89.8177	−304.144	149.764	0	0	1.6
2.5	31.0784	−196.57	97.1029	0	0	8.3
2.7	1102.05	−3651.9	4149.49	−2036.31	367.774	2.4
3.0	736.428	−2474.45	2716.52	−1251.53	207.608	8.8

(b)

a_j	b_0^j/ kcal mol^{-1} Å^{-j}	b_1^j/| kcal mol^{-1} Å$^{-(j+1)}$	b_2^j/ kcal mol^{-1} Å$^{-(j+2)}$	b_3^j/ kcal mol^{-1} Å$^{-(j+3)}$
a_0/kcal mol^{-1}	686741	−796927	306285	−38955.1
a_1/kcal mol^{-1} Å^{-1}	-2.18581×10^6	-2.95658×10^6	1.13764×10^6	−144843
a_2/kcal mol^{-1} Å^{-2}	-1.27855×10^6	1.48664×10^6	−572406	72926.9
a_4/kcal mol^{-1} Å^{-4}	233641	−271783	104697	−13346.7

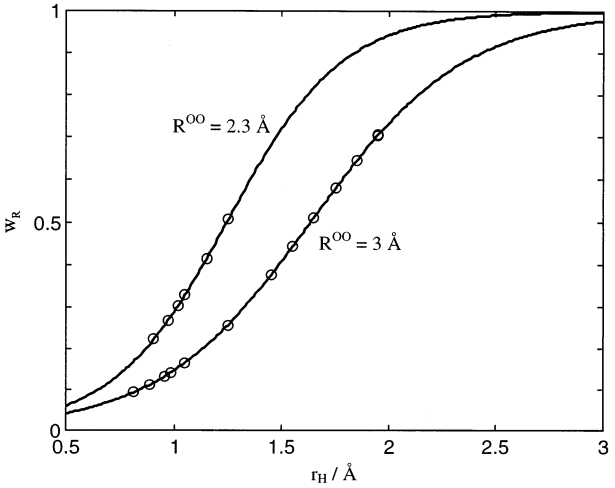

Figure 3. Switching function for interpolation of reactant and product state as a function of the distance of the transferring proton to the carbonyl oxygen atom. Plots are shown for two different oxygen distances R_{OO}.

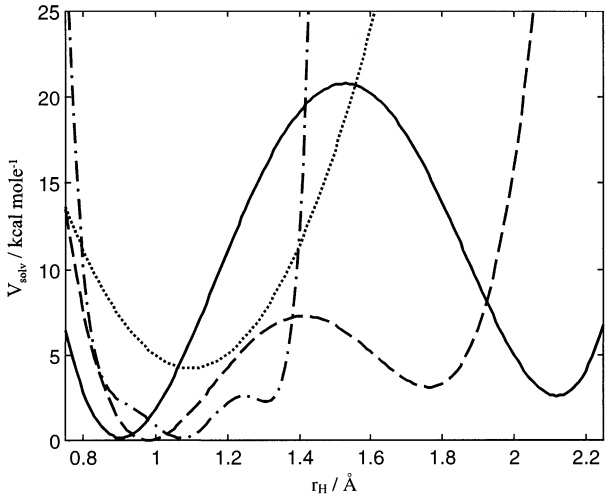

Figure 4. Potential energy surface for proton transport in aqueous solution as a function of the distance of the transferring proton to the carbonyl oxygen atom for selected oxygen distances (R_{OO}: 3.0, 2.7, 2.5, and 2.3 Å: solid, dashed, dash−dotted, and dotted lines).

reactant and product states is determined as −2.5 kcal/mol, and the activation energy for protonation of the amide is about 0.5 kcal/mol. It is also interesting to monitor the distance of the oxygen atoms between the proton is transferred. Figure 5b shows R_{OO} for the minimum energy path as a function of r_H.

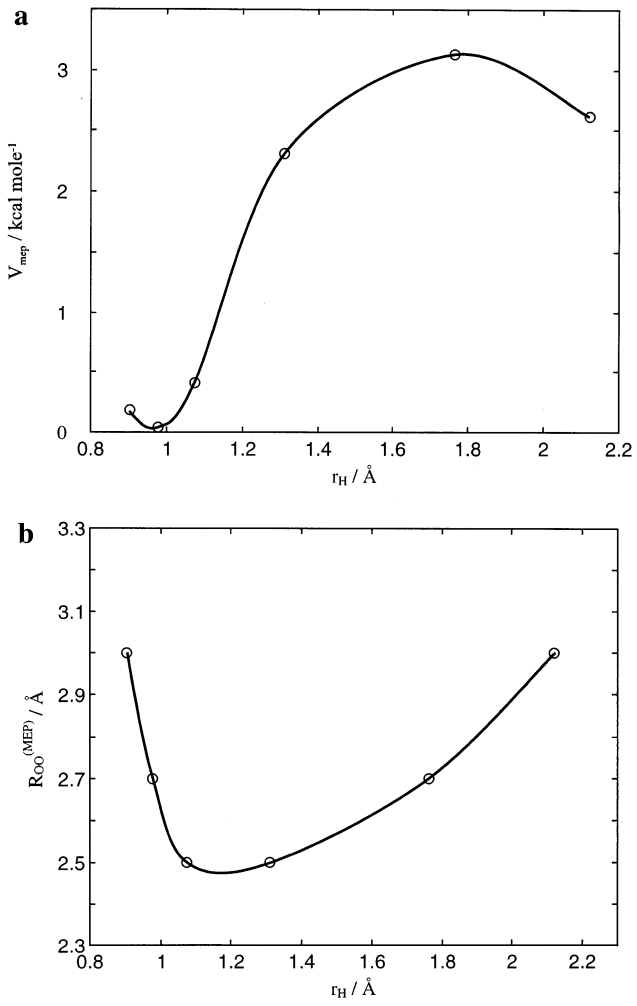

Figure 5. (a) Total potential energy for the minimum energy path as a function of the distance of the transferring proton from the carbonyl oxygen atom. (b) Distance of the oxygen atoms for the minimum energy path as a function of the distance of the transferring proton from the carbonyl oxygen atom.

Accordingly, the oxygen atoms are at distances of 2.7−3.0 Å for both reactant and product states. In the transition state, the oxygen distance was found to be 2.5 Å. In our model, proton transfer from the hydronium ion to NMAA occurs as a three step process: (i) the approaching of an hydronium ion to the carbonyl group up to an oxygen distance of 2.5 Å followed by (ii) proton transfer between the oxygen atoms and finally (iii) the displacement of the product molecules.

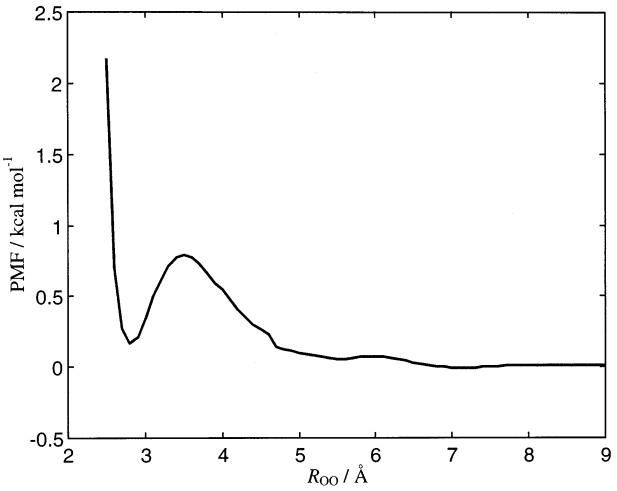

Figure 6. Potential of mean force for the association of a hydronium ion to the model peptide in aqueous solution. The curve is shown as a function of the distance of the oxygen atoms.

At this point, we emphasize that the reactant states derived from Figure 4 are only some of a manifold of possible reactant states. In aqueous solution, the hydrated proton related to the reactant state is not necessarily associated to the first solvent shell of the carbonyl oxygen atom. To elucidate the proton transport from bulk water to the first solvent shell of the peptide, we employed a new hybrid algorithm combining Monte Carlo sampling of solute−solute interactions with a RISM integral equation liquid.[32] By this means, the corresponding potential of mean force for the association of a hydronium ion to a NMAA molecule in aqueous solution was calculated. The reaction coordinate was taken as the distance of the oxygen atoms of the hydronium ion and the carbonyl group of the peptide. The resulting potential of mean force is shown in Figure 6. Accordingly, the association of a hydrated proton to the first solvent shell of the NMAA oxygen atom is related to a difference in free energy of 0.16 kcal/mol only.

5. Conclusion

We presented a quantum/classical calculation of the protonation reaction of the amide oxygen atom of a model peptide. The reaction was investigated in a vacuum and in aqueous solution. In the gas phase, the additional charge was found to be strongly associated to the peptide. A different situation was observed for the transfer process in aqueous solution. The solvent effect increases the probability of finding the excess proton at the water molecule, though peptide protonation is still preferred by about 2.5 kcal/mol.

The solvent effect was modeled using a transferable interpolation scheme. This is accomplished by introducing a switching function, which is used for a smooth transition from reactant to product state. Both states were modeled by classical force fields. This scheme may be applied to estimate the proton transfer potential for various solvent situations. Thus, our results are particularly useful for mixed quantum/classical simulations of amide protonation.

Acknowledgment. K.F. Schmidt and D. Zahn thank the Deutsche Forschungsgemeinschaft (DFG), the DFG Graduiertenkolleg "Kinetik und Mechanismen von Ionenreaktionen", and the Verband der chemischen Industrie (VCI) for financial support.

References and Notes

(1) Mathews, C. K.; van Holde, K. E. *Biochemistry*; Benjamin/Cummings Publ.: Redwood City, CA, 1990.
(2) Zhang, K.; Zimmerman, D. M.; Chung-Phillips, A.; Casssady, C. J. *J. Am. Chem. Soc.* **1993**, *115*, 10812.
(3) Hodoscek, M.; Hadzi, D. *J. Mol. Struct.* **1989**, *194*, 191.
(4) Schmidt, R. G.; Brickmann, J. *J. Solid State Ionics* **1995**, *77*, 9.
(5) Schmidt, R. G.; Brickmann, J. *Ber. Bunsen-Ges. Phys. Chem.* **1997**, *101*, 11166.
(6) Agmon, N. *Isr. J. Chem.* **1999**, *39*, 493.
(7) Hansen, J. P.; McDonald, I. R. *Theory of simple liquids*; Academic Press: London, 1980.
(8) Zahn, D.; Brickmann, J. *Isr. J. Chem.* **1999**, *39*, 483.
(9) Vuilleumier, R.; Borgis, D. *Chem. Phys. Lett.* **1998**, *284*, 71.
(10) Hammes-Schiffer, S. *J. Chem. Phys.* **1996**, *105*, 2236.
(11) Chandler, D.; Andersen, H. C. *J. Chem. Phys.* **1972**, *57*, 1930.
(12) Hirata, F.; Rossky, P. J. *Chem. Phys. Lett.* **1981**, *83*, 329.
(13) Enciso, E. *Mol. Phys.* **1985**, *56*, 129.
(14) Chiles, R. A.; Rossky, P. J. *J. Am. Chem. Soc.* **1984**, *106*, 6867.
(15) Pettitt, B. M.; Karplus, M. *Chem. Phys. Lett.* **1987**, *136*, 383.
(16) Zichi, D. A.; Rossky, P. J. *J. Chem. Phys.* **1986**, *84*, 1712.
(17) Lee, P. H.; Maggiora, G. M. *J. Phys. Chem.* **1993**, *97*, 10175.
(18) Svensson, B.; Woodward, C. E. *J. Phys. Chem.* **1995**, *99*, 1614.
(19) Kawata, M.; Ten-no, S.; Kato, S.; Hirata, F. *J. Phys. Chem.* **1996**, *100*, 1111.
(20) Eu, B. C.; Rah, K. *J. Chem. Phys.* **1999**, *111*, 3327.
(21) von Solms, N.; Chiew, Y. C. *J. Chem. Phys.* **1999**, *111*, 4839.
(22) Fries, P. H.; Patey, G. N. *J. Chem. Phys.* **1985**, *82*, 429.
(23) Singer, S. J.; Chandler, D. *Mol. Phys.* **1985**, *55*, 621.
(24) Frisch, M. J.; Trucks, G. W.; Schlegel, H. B.; Gill, P. M. W.; Johnson, B. G.; Robb, M. A.; Cheeseman, J. R.; Keith, T.; Petersson, G. A.; Montgomery, J. A.; Raghavachari, K.; Al-Laham, M. A.; Zakrzewski, V. G.; Ortiz, J. V.; Foresman, J. B.; Cioslowski, J.; Stefanov, B. B.; Nanayakkara, A.; Challacombe, M.; Peng, C. Y.; Ayala, P. Y.; Chen, W.; Wong, M. W.; Andres, J. L.; Replogle, E. S.; Gomperts, R.; Martin, R. L.; Fox, D. J.; Binkley, J. S.; Defrees, D. J.; Baker, J.; Stewart, J. P.; Head-Gordon, M.; Gonzalez, C.; Pople, J. A. *Gaussian 94*, revision D.4; Gaussian, Inc.: Pittsburgh, PA, 1995.
(25) Becke, A. D. *J. Chem. Phys.* **1993**, *98*, 5648.
(26) Lee, C.; Yang, W.; Parr, R. G. *Phys. Rev. B.* **1998**, *37*, 785.
(27) Jorgensen, W. L. *J. Am. Chem. Soc.* **1996**, *118*, 11225.
(28) Jorgensen, W. L.; Chandrasekhar, J.; Madura, J. D.; Impey, R. W.; Klein, M. L. *J. Chem. Phys.* **1983**, *79*, 926.
(29) Kovalenko, A.; Ten-no, S.; Hirata, F. *J. Comput. Chem.* **1999**, *20*, 928.
(30) Talman, J. D. *J. Comput. Phys.* **1978**, *29*, 35.
(31) Lobaugh, J.; Voth, G. A. *J. Chem. Phys.* **1996**, *104*, 2056.
(32) Schmidt, K. F.; Kast, S. M. *J. Phys. Chem. B* Submitted for publication.